

Supplementary information

Asymmetric coordination activated lattice oxygen in perovskite ferrites for selective anaerobic oxidation of methane

Wenxi Chang^{a,b,†}, Yuming Gao^{c,†}, Jiahui He^{a,b}, Xue Xia^{a,b}, Chuande Huang^{a,*}, Yue Hu^{a,d}, Weibin Xu^{a,d}, Bo Jiang^{c,*}, Yujia Han^{a,d}, Yanyan Zhu^{b,*}, Xiaodong Wang^{a,*}

^aCAS Key Laboratory of Science and Technology on Applied Catalysis, Dalian Institute of Chemical Physics, Chinese Academy of Sciences, Dalian 116023, China

^bCollege of Chemical Engineering, Northwest University, Xi'an 710069, China

^cKey Laboratory of Ocean Energy Utilization and Energy Conservation of Ministry of Education, Dalian University of Technology, Dalian 116023, China

^dUniversity of Chinese Academy of Sciences, Beijing 100049, China

[†]These authors contributed equally to this work.

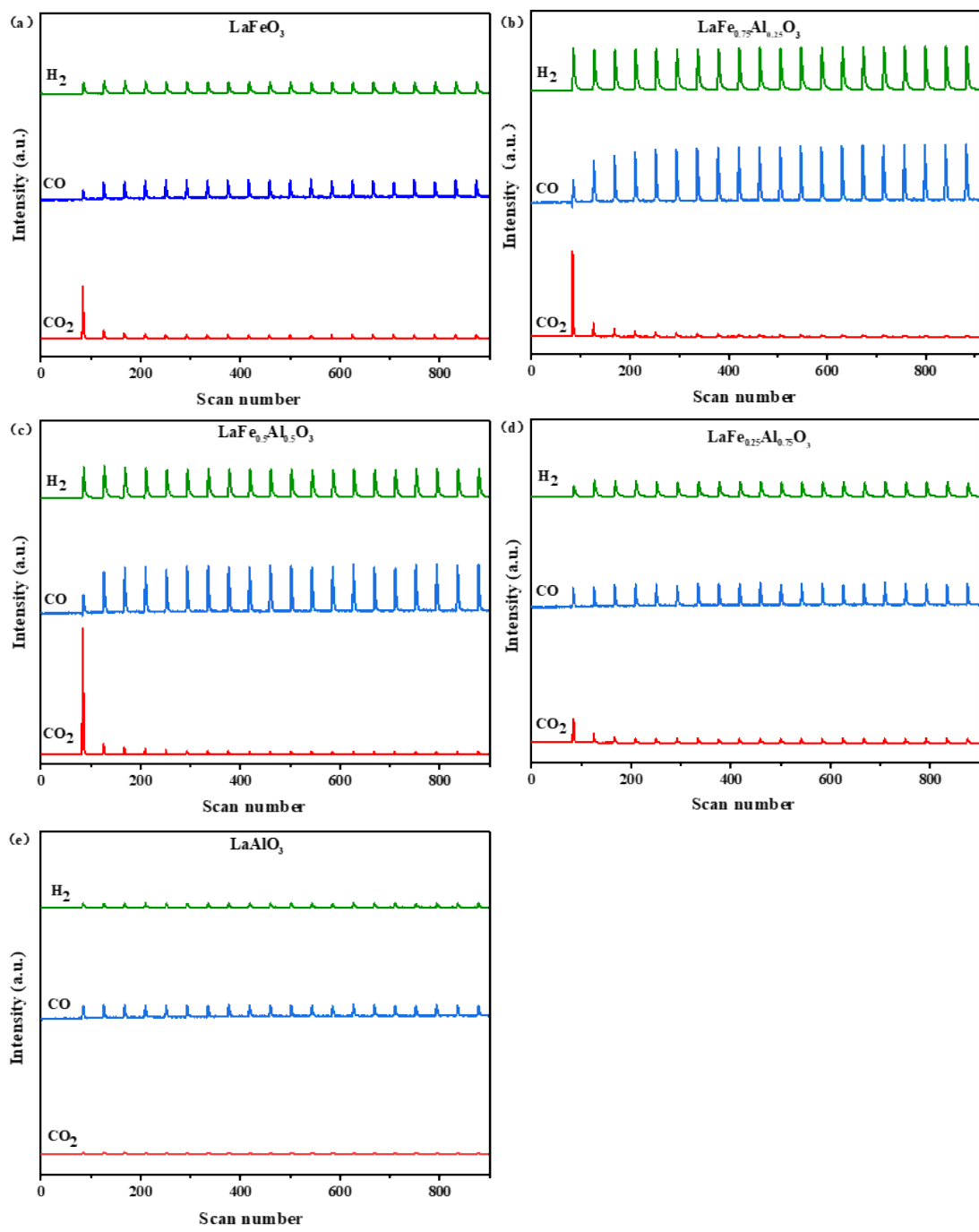


Figure S1. Methane pulse reaction performance over $\text{LaFe}_{1-x}\text{Al}_x\text{O}_3$ ($0 \leq x \leq 1.0$) oxides at 700°C .

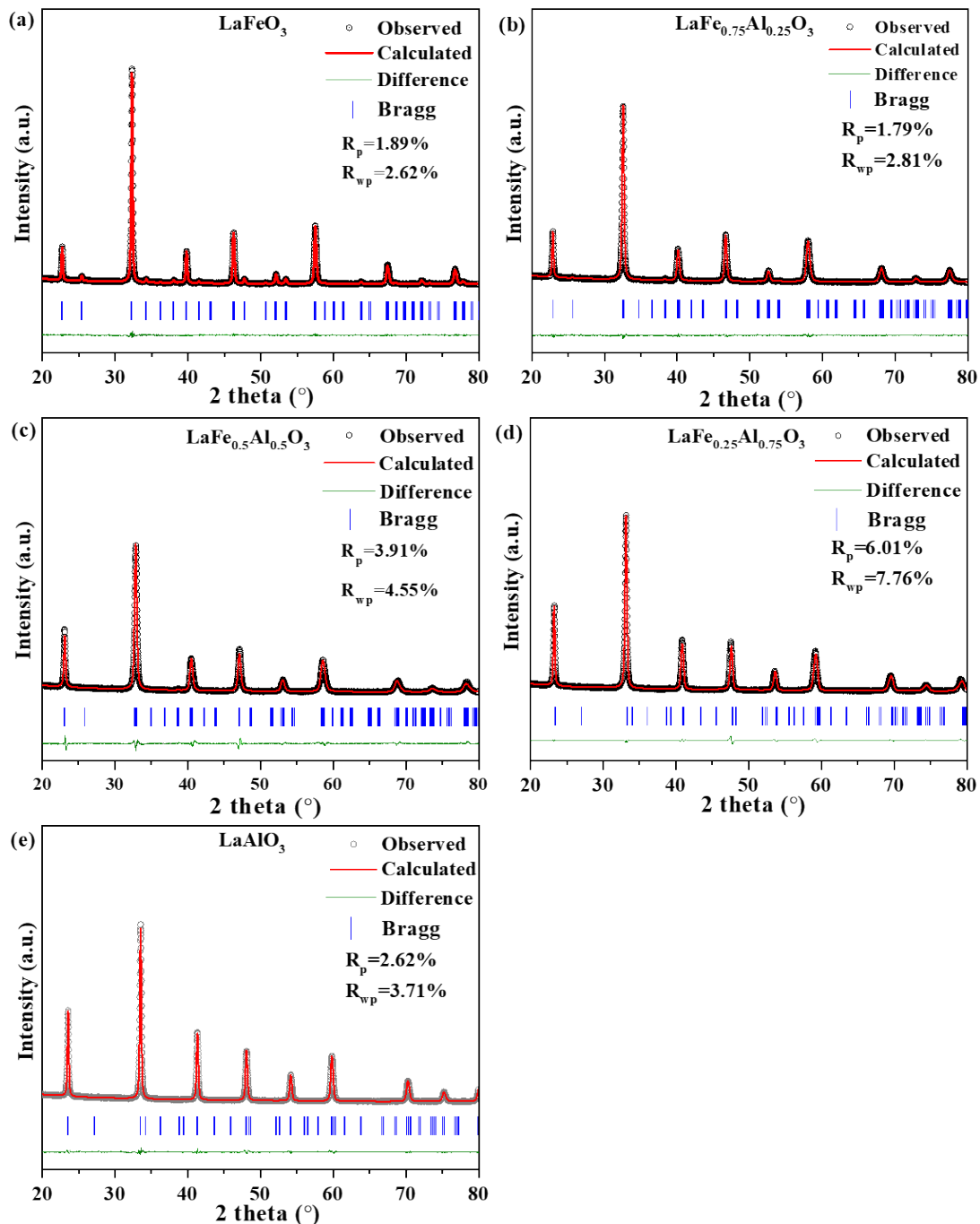


Figure S2. Rietveld refinement results of $\text{LaFe}_{1-x}\text{Al}_x\text{O}_3$ ($0 \leq x \leq 1.0$) oxides.

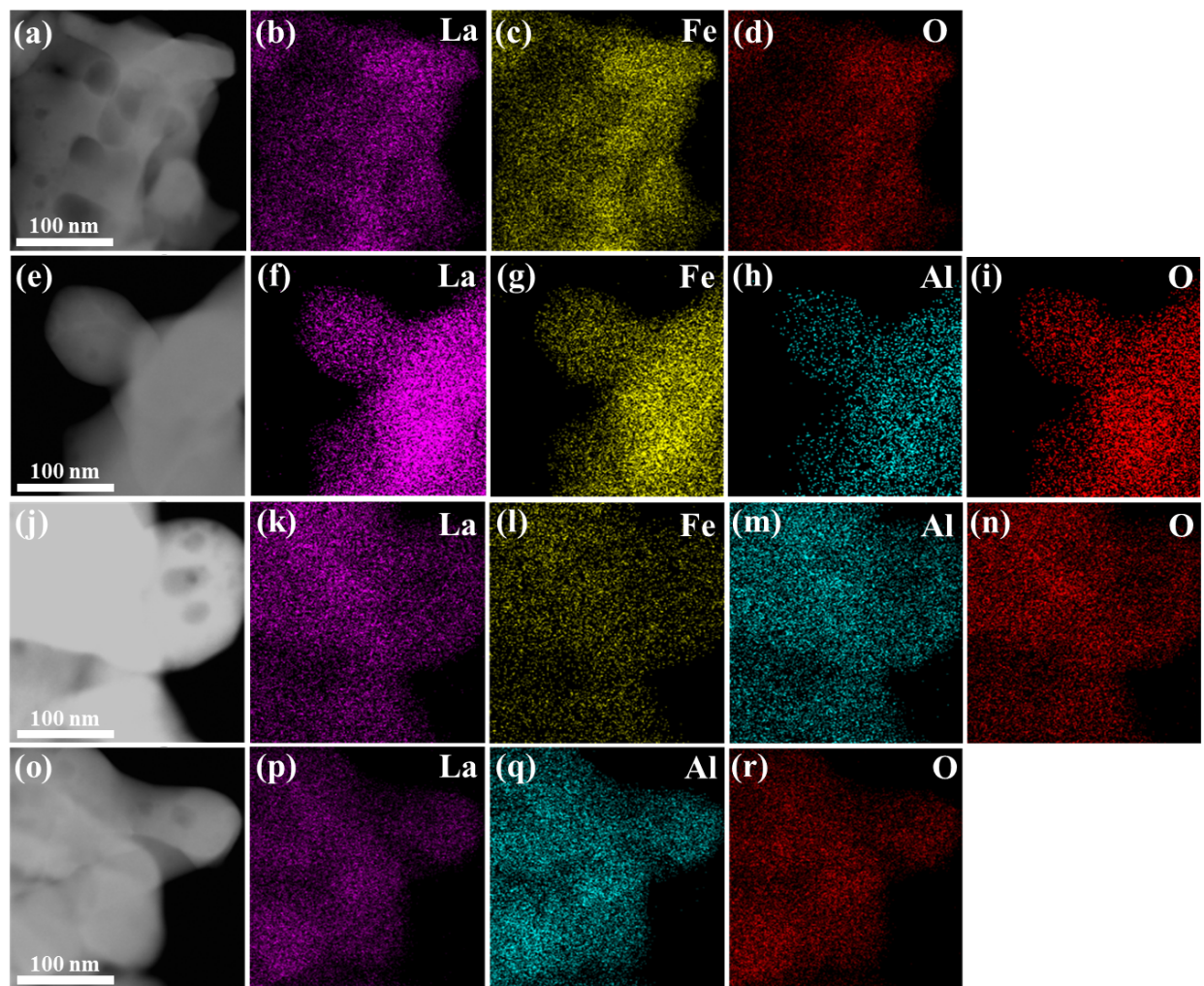


Figure S3. STEM images and corresponding element distribution of (a-d) LaFeO_3 , (e-i) $\text{LaFe}_{0.75}\text{Al}_{0.25}\text{O}_3$, (j-n) $\text{LaFe}_{0.25}\text{Al}_{0.75}\text{O}_3$, and (o-r) LaAlO_3 .

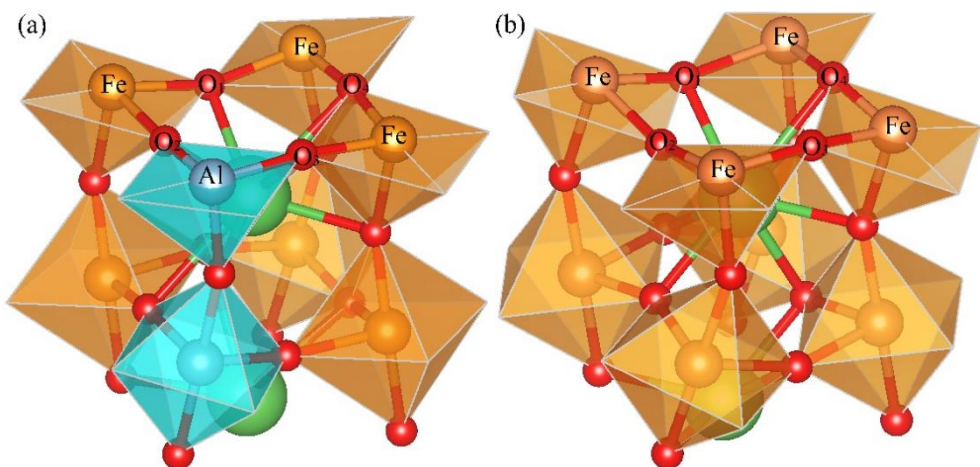


Figure S4. Schematic representations of local structures around Fe on (a) $\text{LaFe}_{0.5}\text{Al}_{0.5}\text{O}_3$ and (b) LaFeO_3 .

Table S1. Basic Parameters for LaFe_{1-x}Al_xO₃ (0 ≤ x ≤ 1) Oxides

Samples	LaFeO ₃	LaFe _{0.75} Al _{0.25} O ₃	LaFe _{0.5} Al _{0.5} O ₃	LaFe _{0.25} Al _{0.75} O ₃	LaAlO ₃
Space Group	Pnma	Pnma	Pnma	R-3ch	R-3ch
Lattice	a= 5.5640	a= 5.4975	a= 5.4550	a= 5.3811	a= 5.3618
Parameters	b= 7.8540	b= 7.7854	b= 7.7289	b= 5.3811	b= 5.3618
(Å)	c= 5.5580	c= 5.5286	c= 5.4831	c= 13.2424	c= 13.1326
Average					
B-O length	2.0037	1.9696	1.9489	1.9074	1.8966
(Å)					
Average					
B-O-B Bond angle (°)	159.2	164.7	168.0	174.9	176.3
Surface area (m ² /g)	9.8	7.6	5.5	6.6	9.8

Table S2. Fitted O 1s data for LaFe_{1-x}Al_xO₃ ($0 \leq x \leq 1.0$) oxides.

Samples	Binding energy (eV)		Ratio of O _A / O _L
	O _A	O _L	
x = 0	531.36	529.04	1.23
x = 0.25	531.35	529.13	1.04
x = 0.5	531.37	529.26	0.87
x = 0.75	531.38	529.31	0.66
x = 1.0	531.38	529.34	0.64

Table S3. Symmetry assignment for Raman phonon modes of LaFeO₃.

Raman shift (cm ⁻¹)	Assignment	Atomic motion
139	B _{2g} (1)	A(z), out-of-phase
157	B _{2g} (2)	A(x), out-of-phase
179	A _g (1)	[010] _{pc} FeO ₆ rotation, in-phase
266	A _g (2)	O ₁ x-z plane
294	A _g (3)	[101] _{pc} FeO ₆ bending, in-phase
415	B _{2g} (3)	O-Fe-O scissor like bending
432	A _g (4)	Fe-O stretching

Table S4. Basic parameters for LaFe_{0.5}Al_{0.5}O₃ and LaFeO₃ obtained by DFT calculations

Parameters		LaFe _{0.5} Al _{0.5} O ₃	LaFeO ₃
bond length (Å)	Fe–O ₁	1.96 Å	1.97 Å
	Fe–O ₂	2.02 Å	2.10 Å
	Fe–O ₃	1.91 Å	2.10 Å
	Fe–O ₄	1.89 Å	1.89 Å
	average	1.95 Å	2.02 Å
bond angle (deg)	Fe–O ₁ –Fe	159.88	158.80
	Fe–O ₂ –Fe	172.53	158.80
	Fe–O ₃ –Fe	172.54	162.31
	Fe–O ₄ –Fe	172.22	162.31
	average	169.30	160.55

Table S5. Calculated stability of chemisorbed $^*\text{CH}_3$ and $^*\text{H}$ on Fe-O or Al-O of Fe-O-Fe and Fe-O-Al motif.

Interaction	Energy (eV)
$^*\text{CH}_3$ on Fe and $^*\text{H}$ on O of Fe-O-Fe	-3.21
$^*\text{CH}_3$ on Fe and $^*\text{H}$ on O of Fe-O-Al	-3.71
$^*\text{CH}_3$ on Al and $^*\text{H}$ on O of Fe-O-Al	-1.72